Scientific Research Publishing

American Journal of Computational Mathematics, 2022, 12, 349-354
https://www.scirp.org/journal/ajcm
ISSN Online: 2161-1211
ISSN Print: 2161-1203

Impact of a Mobile Void within a Charge Distribution on the Electric Field

Haiduke Sarafian

The Pennsylvania State University, University College, York, USA
Email: has2@psu.edu

How to cite this paper: Sarafian, H. (2022) Impact of a Mobile Void within a Charge Distribution on the Electric Field. *American Journal of Computational Mathematics*, **12**, 349-354.
https://doi.org/10.4236/ajcm.2022.124025

Received: October 28, 2022
Accepted: December 17, 2022
Published: December 20, 2022

Abstract

The electric field of a 3D spherical uniform charge distribution embodying a spherical *mobile* void at an exterior point is calculated. The size of the void and its path is arbitrary. Specifically, three different trajectories are analyzed. The movement of the void impacts the electric field so that the field becomes time-dependent. In terms of the chosen path and the size of the bubble, we evaluate the time-dependent electric field. The time profile of the field is calculated. Because of the computational challenges, the most of calculation is carried out utilizing a Computer Algebra System (CAS), specifically *Mathematica* [1]. This project makes the CAS an essential tool not only for calculating the field but for animating the features of the mobile void. An atlas of the study cases is included.

Keywords

Bubble in a Charge Distribution, Electric Field, Computer Algebra System, *Mathematica*

1. Introduction

Figure 1 depicts the problem at hand. As shown, the blue marked circle is the boundary of the spherical charge distribution. It contains a net charge, $+Q$ which is evenly distributed within the sphere of radius R, e.g. $R = 5$ units. Within this sphere there is a void colored pink of radius r; $r < R$. The bubble may move within the sphere on an arbitrary path. Point A is an exterior point of interest. We wish to calculate the electric field, $\boldsymbol{E}$ at A. Since at point A each sphere acts as a point charge with the concentrated charge at their respective centers, first we get the field of the large sphere, and then we treat the void as a uniform charge distribution with a net *negative*, $-Q'$, charge. Since both spheres contain charges with even distributions this yields the charge within the bubble to, $Q' =$

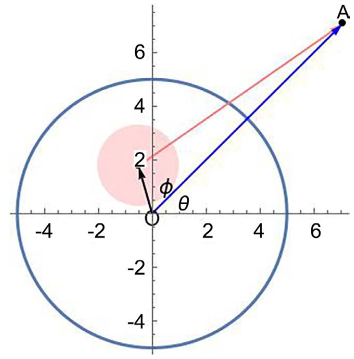

Figure 1. A spherical charge distribution with a blue circular boundary and a void in pink within.

$Q(r/R)^3$. The blue arrow connects the origin to A, and $\boldsymbol{r}_1$ shown with the black arrow connects the origin to the center of the void, and the pink arrow connects the center of the void to A, *i.e.* $\Delta\boldsymbol{r} = \boldsymbol{r}_A - \boldsymbol{r}_1$. Hence the electric field at A becomes [2] [3],

$$\boldsymbol{E}_A = kQ\frac{\boldsymbol{r}_A}{r_A^3} + kQ'\frac{\Delta\boldsymbol{r}}{|\Delta\boldsymbol{r}|^3}, \tag{1}$$

2. Formulation and Analysis

As shown, the $\boldsymbol{E}_A$ contains two vector fields. The field from the large sphere, R is along the extension of the blue arrow, while the field from the pink is along the opposite direction of the pink arrow. A combination of these two vectors is given by (1), where $k = 1/(4\pi\epsilon_0) = 9\times10^9$, SI units. Breaking the vectors of interest in horizontal and vertical components gives,

$$\boldsymbol{r}_A = r_A\cos[\theta]\hat{i} + r_A\sin[\theta]\hat{j}, \tag{2}$$

$$\Delta\boldsymbol{r} = \left(r_A\cos[\theta]\hat{i} + r_A\sin[\theta]\hat{j}\right) - \left(r_1\cos[\phi]\hat{i} + r_1\sin[\phi]\hat{j}\right), \tag{3}$$

where θ and ϕ, are the angles between the $\boldsymbol{r}_A$ and $\boldsymbol{r}_1$ with the horizontal axis. This gives,

$$|\Delta\boldsymbol{r}|^3 = \left(r_A^2 + r_1^2 - 2r_Ar_1\cos[\theta-\phi]\right)^{\frac{3}{2}}, \tag{4}$$

Substituting (4) in (1) and simplifications yield the components of $\boldsymbol{E}_A$,

$$\frac{E_{Ax}}{kQ} = \frac{1}{r_A^2}\cos[\theta] - \left(\frac{r}{R}\right)^3\frac{1}{|\Delta r|^3}\left(r_A\cos[\theta] - r_1\cos[\phi]\right), \tag{5}$$

$$\frac{E_{Ay}}{kQ} = \frac{1}{r_A^2}\sin[\theta] - \left(\frac{r}{R}\right)^3\frac{1}{|\Delta r|^3}\left(r_A\sin[\theta] - r_1\sin[\phi]\right), \tag{6}$$

The magnitude of $\boldsymbol{E}_A$ and its angular orientation are, respectively

$$E_A = \sqrt{E_{Ax}^2 + E_{Ay}^2}, \tag{7}$$

$$\Theta = \arctan\left[\frac{E_{Ay}}{E_{Ax}}\right], \tag{8}$$

And since one of our objectives is to analyze the impact of the mobile void, and its relevant impact on the $\boldsymbol{E}$, we set the value of $kQ = 1$. Our study falls into one of three categories.

Case 1. The bubble has the size half of the size of the radius of charge distribution, e.g. $r = 1/2R$. The simplest scenario is when point A is along the extension of the radial vector and the center of the void and the center of the spherical charge are aligned. This is shown in Figure 2.

In this situation as shown in Figure 2 angles, θ and ϕ overlap. The E_A becomes,

$$E_A = \frac{1}{r_A^2} - \frac{1}{8}\frac{1}{\left(r_A - \frac{R}{2}\right)^2}, \tag{9}$$

Here we consider a static condition where the void is stationary. The field at A is time-independent and is given by (9). The extension of this case is a scenario where the void is smaller than the case discussed. The formulation is straightforward, the situation is depicted in Figure 3.

Case 2. This case deals with either a displaced A that comes about by moving the observation point A around the initial position and/or preferably by circulating the void around the center of the charge distribution, as shown in Figure 4. Either one of these scenarios has an implication, the said vectors become misaligned making $\theta \neq \phi$. Here, (5) and (6) become active.

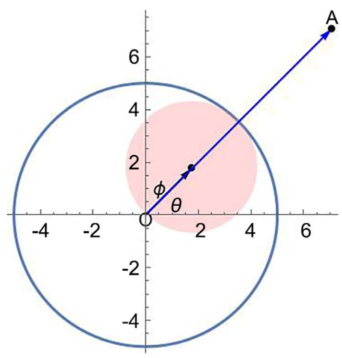

Figure 2. The center of the large charge distribution, O, and the center of the void is aligned.

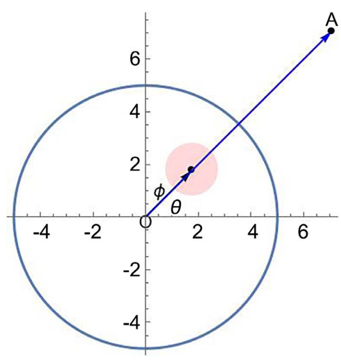

Figure 3. The void is arbitrarily smaller. The center of the void and the observation point A are aligned.

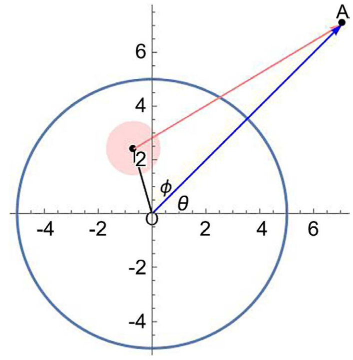

Figure 4. A spherical bubble manually is moved about the center, O. The radial position vectors are misaligned as shown with two different angles, θ, and ϕ.

In **Figure 4**, we show a situation where $r < 1/2R$. Of course the size of the bubble may be adjusted at will. For the given situation and chosen angles θ and ϕ, (5) and (6) give the components of the E_A. Instead of giving a set of numeric values for field components because in the forthcoming case 3, here we would rather postpone the numeric calculation.

Case 3a. The impact of the mobile bubble

Here we consider a situation where the void is mobile. We have set the formulation of the problem such that any kind of path could be handled. For the sake of demonstration only here we consider a situation where the bubble circulates at a constant pace around the center of the charge distribution. To achieve this goal we replace the static orientation angle, θ with a time-dependent entity, *i.e.* $\theta \to \omega t$. Where ω is the angular speed, $\omega = 2\pi ft$ with the frequency f at our disposal. The trajectory of the orbital motion is shown in **Figure 5**.

The far-right figure is a snapshot of the animation. If the animation could have been activated one could see the circulating bubble around the center tracing the shown pink circle. We notice the powerful CAS's usefulness. Without it, these would have been a long computational procedure.

Case 3b. The impact of the oscillating-circulating mobile bubble

As pointed the bubble may move on an arbitrary path. To make the situation just a tad challenging here we consider a situation where the bubble with its constant radius not only circulates about the center, O but simultaneously oscillates along the position vector r_1. This is implemented by replacing the constant ϕ with $\phi \to 2\pi f_\phi t$. Here f_ϕ is the frequency of the oscillating void along its radial direction. We noticed this situation somewhat resembles the Lissajous [4] phenomenon. Here we demonstrate two different examples. First we set the $\{\theta, \phi\}$ = $(2\pi\ 1\ t, 2\pi\ 3\ t\}$ and $\{\theta, \phi\} = \{2\pi\ 1\ t, 2\pi\ 5\ t\}$, respectively. For the former case, the ratio $\theta/\phi = 1/3$ and for the latter $\theta/\phi = 1/5$. These ratios control the number of peddles in the carnation shown by the pink paths. **Figure 6** is associated with the first and **Figure 7** with the second ratio, respectively.

In **Figure 6** and **Figure 7**, the far left drawings have overlapped curves, *i.e.* the blue-green appears green.

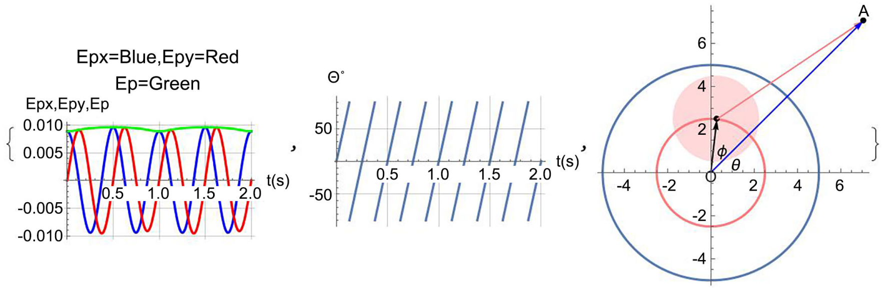

Figure 5. The pink circular orbit in the far end drawing is the path of the center of the void. The pink circle is the void. The far left and the middle graphs are the x and y components of the field at A and the angular fluctuation of the orientation of the field vs time, t, respectively.

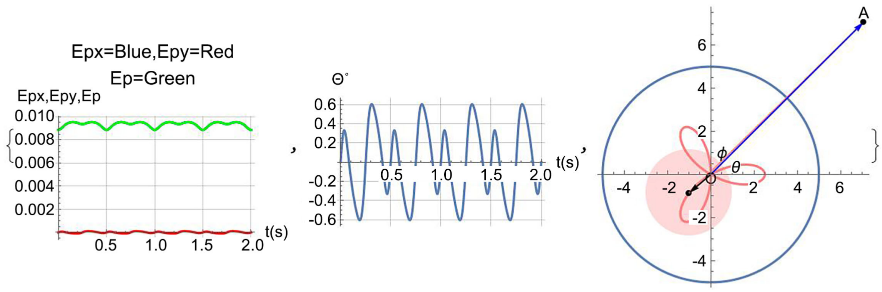

Figure 6. The description is the same as in **Figure 5**. The three peddle-carnation is shown in pink on the far end drawing associated with the $\theta/\phi = 1/3$.

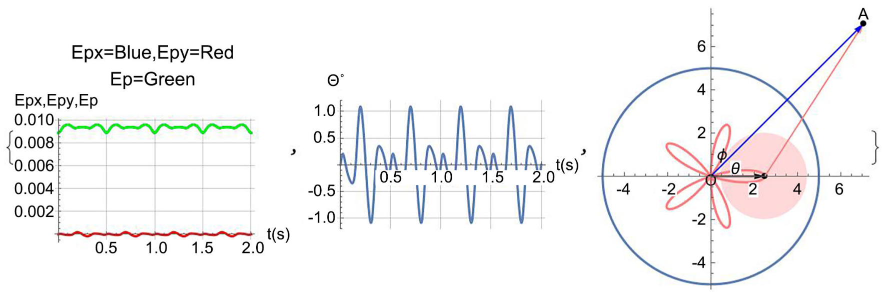

Figure 7. A description is the same as **Figure 5**. The five peddle-carnation is shown in pink on the far end drawing associated with the $\theta/\phi = 1/5$.

3. Conclusions and Comments

We begin this project thinking about how to handle the impact of a void in a chosen charge distribution. In the course of analyzing the problem not only we addressed the issue but ended up expanding the problem from a static situation to a dynamic one. Our analysis handles the impact of a mobile bubble within a charge distribution. A few cases are presented. At some point, the mobility of the void is related to that of the Lissajous curves. The presented analysis has the potential to be extended even more, e.g. multiple bubbles with arbitrary pathways. The kinematics of the mobile voids is totally under our control. *Mathematica* can achieve the set goals. Although the presented article focuses only on the static aspect of the proposed scenario, the author enjoyed watching the animations. The learned lesson is priceless. The interested reader may find [5] [6] resourceful for making the reported graphs, calculations, and animations.

Acknowledgements

The author acknowledges the John T. and Page S. Smith Professorship funds for completing and publishing this work.

Conflicts of Interest

The author declares no conflicts of interest regarding the publication of this paper.

References

[1] Mathematica V13.1. http://Wolfram.com

[2] Ohanian, H. (1989) Physics. 2nd Edition Expanded, W.W. Norton, New York.

[3] Jackson, J.D. (1999) Classical Electrodynamics. 3rd Edition, John Wiley & Sons, Inc., New Jersey.

[4] https://en.wikipedia.org/wiki/MIT_Lincoln_Laboratory

[5] Wolfram, S. (1996) *Mathematica* Book. 3rd Edition, Cambridge University Press, Cambridge.

[6] Sarafian, H. (2019) *Mathematica* Graphics Examples. 2nd Edition, Scientific Research Publishing, Wuhan.